Available online at www.sciencedirect.com

SCIENCE DIRECT®

Sedimentary Geology 169 (2004) 175–189

Sedimentary Geology

www.elsevier.com/locate/sedgeo

Optical dating of deep-sea sediments using single grains of quartz: a comparison with radiocarbon

J.M. Olley[a,*], P. De Deckker[b], R.G. Roberts[c], L.K. Fifield[d], H. Yoshida[c], G. Hancock[a]

[a] CSIRO Land and Water, PO Box 1666, Canberra ACT 2601, Australia
[b] Department of Earth and Marine Sciences, The Australian National University, Canberra ACT 0200, Australia
[c] GeoQuEST Research School, School of Earth and Environmental Sciences, University of Wollongong, Wollongong NSW 2522, Australia
[d] Department of Nuclear Physics, Research School of Physical Sciences and Engineering, The Australian National University, Canberra ACT 0200, Australia

Received 21 November 2003; received in revised form 31 March 2004; accepted 13 May 2004

Abstract

In this paper, we demonstrate that optical dating of single grains of quartz offers an alternative means of dating deep-sea sediments. The precision and accuracy of the technique, which has the potential to date sediments deposited during the last 500,000 years or so, is limited by the random and systematic uncertainties associated with producing optical ages. These result in total relative age uncertainties of between 10% and 20% at the 68% confidence interval, which are similar in size to those associated with Late Quaternary oxygen-isotope chronologies. We analysed single grains of quartz from several depth intervals down core Fr10/95-GC17, which was collected offshore from Cape Range Peninsula, Western Australia, from a water depth of 1093 m in the eastern Indian Ocean. The single-grain optical ages are shown to be consistent with AMS radiocarbon ages obtained from planktonic foraminifera from the same core. We also show that marine sediments are not immune from partial or heterogeneous bleaching (incomplete resetting) of the optical dating signal. Where partial or heterogeneous bleaching of the optical dating signal is indicated, we recommend that single-grain dating be employed and the burial dose estimated from the population of grains with the lowest absorbed radiation dose.

Keywords: Geochronology; Luminescence; Optical dating; Single grains; Radiocarbon; Indian Ocean; Deep-sea core; Palaeoceanography; Late Quaternary

1. Introduction

Deep-sea sediment cores are important sources of palaeoenvironmental information, but dating of such sediments remains problematic. Accelerator Mass Spectrometry radiocarbon (AMS ^{14}C) dating is limited to organic materials younger than about 50,000–60,000 years, and uncertainties of up to several millennia remain in converting ^{14}C ages to calendar-year ages due to temporal variations in atmospheric ^{14}C concentrations (e.g., Laj et al., 2002; Hughen et al., 2004) and the marine carbon reservoir (Sikes et al., 2000). Application of uranium–thorium (U/Th) radionuclide techniques, which can extend well beyond the limit of ^{14}C dating, is complicated by the presence of variable amounts of initial ^{230}Th (Henderson and Slowey, 2000). Chronologies developed

* Corresponding author.
E-mail address: Jon.Olley@csiro.au (J.M. Olley).

0037-0738/$ - see front matter © 2004 Elsevier B.V. All rights reserved.
doi:10.1016/j.sedgeo.2004.05.005

by tuning of global ice volume, as recorded by marine oxygen-isotopes, to changes in the Earth's orbit (Martinson et al., 1987) are dependent on the assumed model of climate change. If this model is wrong, then the chronology may be inadequate (Henderson and Slowey, 2000). Current estimates of the total uncertainty associated with oxygen-isotope chronologies are frequently of the order of 5000–10,000 years over the last 300,000 years (Martinson et al., 1987). A dating technique is needed that (a) is not linked to models of past climate change; (b) is independent of variations in the marine carbon reservoir; (c) is able to date events that occurred before and after 50,000–60,000 years ago; and (d) is independent of variations in the chemistry of deep-sea sediments.

Deep-sea sediments were one of the first types of natural deposit investigated using luminescence dating (Wintle and Huntley, 1979, 1980; Berger et al., 1984). But a variety of uncertainties, including the adequacy of exposure of the sediments to sunlight at the time of deposition, discouraged the widespread application of thermoluminescence (TL) dating techniques to marine sediments (Stokes et al., 2003). The subsequent development of optical dating (Huntley et al., 1985; Aitken, 1998) has enabled the most light-sensitive signals from quartz and feldspar to be selectively exploited, and this has incited interest in using the optically stimulated luminescence (OSL) signals to obtain burial ages for deep-sea sediments. Stokes et al. (2003) recently proposed that optical dating of multiple-grain aliquots of silt-sized quartz could be used to provide depositional ages for deep-sea sediments. They examined two independently dated sediment cores from the northwestern Indian Ocean (~300 km from the nearest landmass and >3000 m water depth). The nine optical ages produced during that study agreed well with the independent chronologies and had reported relative standard errors of 3–6% on ages ranging from 7000 to 117,000 years.

1.1. Optical dating

Optical dating relies on the fact that, when buried, quartz grains begin to accumulate a trapped-charge population that increases in a measurable and predictable way in response to the ionising radiation dose to which the grains are exposed. Exposure to sunlight releases the light-sensitive trapped charge, thereby resetting the OSL signal; a process commonly referred to as 'bleaching'. The time elapsed since sediment grains were last exposed to sunlight may be estimated by measuring the OSL signal from a sample of sediment, determining the equivalent dose (D_e) that this represents (for which the SI unit is the gray, Gy), and estimating the rate of exposure of the grains to ionising radiation averaged over the period of burial. The latter parameter of interest is termed the dose rate (D_r). The burial age of well-bleached grains may then be obtained from the following equation:

$$\text{Burial age} = D_e/D_r$$

The OSL signal of clean quartz grains exposed directly to sunlight is reduced to a negligible level within a few seconds (Aitken, 1998; Wintle, 1997). However, incomplete or non-uniform bleaching is commonplace in many depositional environments (Murray and Olley, 2002), due to surface coatings on the grains and/or insufficient exposure to sunlight during sediment transport. This results in grains being deposited with a heterogeneous distribution of residual trapped charge, and a correspondingly wide range of measured D_e values. For such sediments, the population of grains with the lowest measured D_e values provides the most accurate estimate of D_b: the burial dose to which those grains that were well bleached at deposition have been exposed since the most recent transport event (Olley et al., 1998, 1999, in press).

1.2. This study

Stokes et al. (2003) examined aliquots of quartz that consisted of many thousands of silt-sized grains. Aliquots composed of such a large number of grains would be expected to mask any evidence of partial bleaching (Olley et al., 1999), yet the authors reported that a small number of aliquots produced D_e values that lay beyond three standard deviations of the mean. The cause of the spread in observed D_e values remains unexplained, but its existence suggests that partial or heterogeneous bleaching may be an issue for luminescence dating of deep-sea sediments. Here we examine the extent of partial bleaching of deep-sea

sediments by means of single-grain optical dating, and compare the resulting optical ages to the calibrated ^{14}C chronology obtained for planktonic foraminifera from the same sediment core. The degree of sediment bleaching, the accuracy and precision of the optical ages, and the potential age range for the technique in the marine environment are explored.

2. The study core

Gravity core Fr10/95-GC17 (referred to as GC17 hereafter) was collected from 60 km west of Cape Range Peninsula, northwestern Australia (22°02.74′ S, 113° 30.11′ E), from a water depth of 1093 m in the eastern Indian Ocean. It is one of the most intensively studied deep-sea cores from the Australian region. Past investigations have examined changes in the planktonic foraminifera (Martinez et al., 1999), calcareous nanoplankton (Takahashi and Okada, 2000), clays (Gingele et al., 2001), calcium carbonate percentage (De Deckker, 2001), pollen (van der Kaars and De Deckker, 2002), benthic foraminifera (Murgese, 2003), dinoflagellates (M. Young, in preparation), and organic and inorganic carbon (M. Sloan, unpublished data). All these studies point to the core being one of high quality, suitable for determining patterns of environmental change in both the marine and terrestrial environments, and with no evidence of reworking, or a hiatus in deposition, within the last ~ 45,000 years. The upper 95 cm of the core has a characteristically yellowish brown colour (10YR4/3) and the deeper deposits are typically olive grey in colour (7.5Y5/2). The transition between the two distinct colours occurs over a depth interval of 5 cm, but with no corresponding change in the depositional environment. A total of 15 AMS ^{14}C ages on planktonic foraminifera, which give the most accurate carbon-age for marine sediment horizons (Ohkouchi et al., 2002), provides a chronology for the upper 250 cm of the core (van der Kaars and De Deckker, 2002).

The core site is under the pathway of aeolian dust transported from the Australian mainland (Jennings, 1968; Bowler, 1978), and quartz grains of fine-sand and silt size are present throughout the core. Modern dust storms in Australia move millions of tonnes of sediment (Hesse and McTainsh, 2003), and model results indicate that dust activity during the Last Glacial Maximum was an order-of-magnitude higher than it is today (Harrison et al., 2001). Deposition rates in the eastern Indian Ocean of up to 0.8 mg cm^{-2} $year^{-1}$, or ~ 0.5 cm per 1000 years, are reported to have occurred in the last 50,000 years (Hesse and McTainsh, 2003).

3. Sample descriptions and treatment

Water contents were determined at 2 cm intervals down the core. For the OSL analyses, sediment samples OSL 1 to OSL 7 were collected from depth intervals of 7–8, 57–58, 83–84, 123–124, 139–140, 181–184 and 248.5–251.5 cm, respectively. These horizons had been sampled previously for ^{14}C dating. Sand-sized grains of quartz (60–70 μm in diameter) were extracted from each of the OSL samples using standard purification procedures (e.g., Aitken, 1998). The quartz grains were then etched in 40% hydrofluoric acid for 50 min to remove the outer ~10 μm rinds and to completely remove any whole feldspar grains. Finally, acid-soluble fluorides were removed in 15% hydrochloric acid. Although heavy minerals were not removed by means of density separation, the absence of dark-coloured minerals in the purified extracts was verified by visual inspection of the OSL samples. To test for the presence of heavy minerals, a density separation (at 2.70 g cm^{-3}) was made on a sample composed of material collected from above and below sample OSL 6. Measurements of the lithogenic radionuclide concentrations were made on sediment samples collected from a continuous narrow strip of sediment cut from 7 cm above to 15 cm below the OSL sampling depth for the near-surface sample, and from 15 cm above to 15 cm below for all other OSL samples.

4. Analytical methods

Equivalent doses were determined from measurements of the OSL signals emitted by single grains of quartz. The etched quartz grains were loaded on to aluminium discs (custom-made at CSIRO) that were drilled with a 10 × 10 array of chambers, each of 100 μm depth and 100 μm diameter. The OSL measurements were made on a Risø TL/OSL-DA-15 reader

using a green (532 nm) laser for optical stimulation, and the ultraviolet emissions were detected by an Electron Tubes 9235QA photomultiplier tube fitted with 7.5 mm of Hoya U-340 filter. Laboratory irradiations were conducted using a calibrated $^{90}Sr/^{90}Y$ beta source mounted on the reader. For all of the samples, equivalent doses were determined using a modified single-aliquot regenerative-dose protocol (Olley et al., in press). The OSL signals were measured for 1 s at 125 °C with the laser held at 90% power (i.e., continuous-wave OSL), using a preheat of 240 °C (held for 10 s) for the 'natural' and regenerative doses, and a preheat of 160 °C (held for 10 s) for the test doses (each of 6.0 Gy). The OSL signals induced by the test doses are used to correct for any changes in OSL sensitivity during the natural and regenerative dose cycles. The OSL signals were determined from the initial 0.1 s of data, using the final 0.2 s to estimate the background count rates. Each disc was exposed to infrared (IR) radiation for 40 s at 125 °C before each of the laser stimulations to minimise any contribution to the OSL output from IR-sensitive minerals (e.g., feldspars) internal to the quartz grains (e.g., Huntley et al., 1993). Each grain received a series of regenerative doses (of up to 130 Gy) from which a response curve of OSL intensity versus dose was constructed, including a zero-dose check for the extent of thermal transfer (Aitken, 1998) and a repeat dose point to examine the adequacy of the test dose sensitivity-correction procedure. Grains were rejected if they did not produce a measurable OSL signal in response to the test dose (grains that were accepted produced between 100 and 26,000 counts in response to the test dose, with an average of ~2500 counts); had OSL decay curves that did not reach background after 1 s of laser stimulation (~1% of grains); or, for a further ~1% of grains, produced natural OSL signals that did not intercept the regenerated dose-response curves ('Class 3' grains of Yoshida et al., 2000). The reported D_e uncertainties for each grain are based on counting statistics and curve-fitting uncertainties, including a 3.5% uncertainty (for each OSL measurement) to accommodate the reproducibility with which the laser beam can be positioned (Truscott et al., 2000).

Linearly modulated (LM) OSL measurements were made on 100 separate grains from sample OSL 6 (181–184 cm). This sample showed a wide spread in equivalent doses (7.9 ± 0.7 to 110 ± 20 Gy) measured using continuous-wave stimulation. The OSL signal from quartz consists of a number of components that bleach at different rates (Singarayer et al., 2000; Singarayer and Bailey, 2003, 2004). Comparison of the LM-OSL signals dominated by the fast-to-bleach and slow-to-bleach components provides a means of deducing the degree to which individual quartz grains had been bleached by sunlight prior to deposition (Yoshida et al., 2003). The LM-OSL signals were measured for 30 s at 125 °C with the laser ramped from 0% to 90% power, using the same preheat conditions as above. Net OSL counts for the fast-dominated and slow-dominated LM-OSL components were obtained from the initial 5 s and last 5 s of data, respectively. Background counts were estimated for the same time intervals from a second laser stimulation following each LM-OSL measurement. Following Olley et al. (in press), each disc was also exposed to IR radiation for 40 s at 125 °C before each of the paired (signal and background) laser stimulations.

The dose rates were determined from the radionuclide concentrations in dried and powdered subsamples of sediment, which were analysed using a combination of high-resolution gamma spectrometry for ^{228}Ra, ^{228}Th, ^{226}Ra, ^{210}Pb and ^{40}K (Murray et al., 1987) and alpha-particle spectrometry for ^{238}U, ^{234}U, ^{230}Th and ^{232}Th (Martin and Hancock, 1992). Independent checks on calibration were performed using various standards from Amersham and the U.S. National Bureau of Standards, and from IAEA intercomparisons. Dose rates were calculated using the conversion factors listed in Tables 9–12 of Stokes et al. (2003). The dry dose rates were adjusted for water content, following Aitken (1985), using the average water content of the material 15 cm to either side of each OSL sample to represent the 'as measured' value. The latter was then adjusted to allow for variations in water content during the period of sample burial (due to sediment compaction), using the measured water contents for the overlying sediments and assuming a linear rate of sediment accumulation. In the case of the near-surface sample, the average water content from 0 to 23 cm depth was used. Beta dose attenuation factors were taken from Mejdahl (1979), and the effective internal alpha dose rates were estimated as ~0.03 mGy $year^{-1}$ (similar to values reported previously for Australian quartz grains by Bowler et al., 2003).

5. Results and discussion

5.1. Radiocarbon ages

The 15 AMS ^{14}C ages on planktonic foraminifera belonging to *Globigerinoides sacculifer* are reported in Table 1. The 1σ and 2σ calibrated ^{14}C age ranges are also reported in Table 1, and the 1σ calibrated ages are plotted against sample depth in Fig. 1. The calibrated ^{14}C age ranges for the samples from depths above 140 cm were determined using the marine calibration of Calib 4.3 (Stuiver et al., 1998). For the three samples from depths of between 150 and 250 cm, we have used the calibration dataset of Hughen et al. (2004), which extends the ^{14}C time scale back to 50,000 calendar years before the present. A marine reservoir age of 400 years was subtracted from the conventional (uncalibrated) ^{14}C ages (in Table 1) before calibration. The reported age ranges incorporate both the error on the ^{14}C age and the uncertainty in the calibration.

5.2. Optical ages

5.2.1. Dose rates

The radionuclide concentrations for the samples are summarised in Table 2. In each sample, the measured concentrations of ^{232}Th, ^{228}Ra and ^{228}Th from the thorium decay series are within analytical uncertainty, consistent with the decay chain presently being in secular equilibrium. Consequently, the reported ^{232}Th concentrations listed in Table 2 represent the weighted means of the measured ^{232}Th, ^{228}Ra and ^{228}Th concentrations for each sample. A conspicuous feature of the ^{232}Th-series nuclides is the two to eight times higher concentrations in the upper yellowish brown (10YR4/3) sediments than in the lower olive grey (7.5Y5/2) sediments. A similar pattern is evident in the ^{40}K data, with concentrations in the upper horizons being two to nine times those in the deeper sediments. The higher concentrations of the ^{232}Th-series nuclides and ^{40}K in the upper horizons probably reflect the higher terrigenous clay content of this unit (Gingele et al., 2001).

In the ^{238}U decay series, measured concentrations of ^{230}Th, ^{226}Ra and ^{210}Pb in all of the samples (except the near-surface sample) are consistent with secular equilibrium. The near-surface sample has a ^{210}Pb excess of 12.9 ± 2.3 Bq kg^{-1}, but the decay of ^{210}Pb contributes negligibly to the dose rate. Accordingly, the ^{230}Th results reported in Table 2 are the weighted means of the measured concentrations of ^{230}Th, ^{226}Ra and ^{210}Pb, except for the near-surface sample, for which the reported value is the weighted mean of the measured concentrations of ^{226}Ra and ^{230}Th. The concentrations of ^{234}U are in excess of

Table 1
Sampling depths, laboratory sample codes, conventional AMS ^{14}C ages and calibrated 1σ and 2σ ^{14}C age ranges for planktonic foraminifera from gravity core Fr10/95-GC17

Sampling depth (cm)	Laboratory sample code	Radiocarbon age[a] (years BP)	Calibrated radiocarbon 1σ age range (years)	Calibrated radiocarbon 2σ age range (years)
7–8	ANUA 13031	1630 ± 185	970–1340	790–1550
19–20	ANUA 13030	2150 ± 600	1110–2450	570–3150
45–46	ANUA 13029	4050 ± 225	3800–4390	3510–4680
57–58	ANUA 13028	4760 ± 220	4780–5320	4500–5560
65–66	ANUA 13027	6200 ± 180	6430–6840	6270–7080
75–76	ANUA 13026	7370 ± 190	7640–7990	7480–8180
83–84	ANUA 13025	7930 ± 220	8150–8630	7970–8870
97–98	ANUA 6124	9420 ± 230	9800–10,330	9460–10,790
105–106	ANUA 13024	11,330 ± 260	12,370–13,150	12,050–13,470
117–118	OZD499	13,080 ± 110	14,340–15,400	14,210–15,540
123–124	OZD741	14,300 ± 110	16,300–16,820	16,060–17,090
139–140	OZD744	19,250 ± 280	21,780–22,730	21,360–23,240
149–150	ANUA 13023	20,240 ± 550	21,750–23,900	20,600–24,500
181–184	ANUA 13022	27,820 ± 780	28,900–32,600	28,200–34,000
248.5–251.5	ANUA 13020	40,650 ± 1130	40,200–46,500	38,400–48,000

[a] The ANUA values differ slightly from those reported earlier due to correction for fractionation and the adoption of more realistic errors.

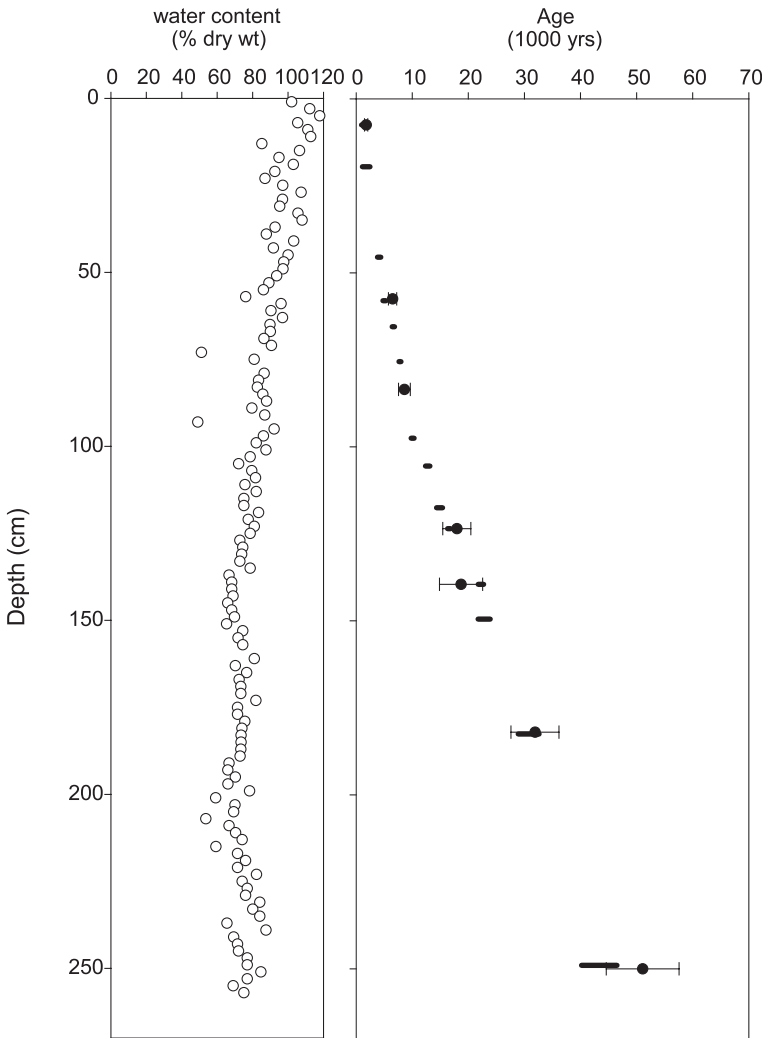

Fig. 1. Measured water contents, calibrated 1σ ^{14}C age ranges (horizontal bars) and optical ages (filled circles and 68% confidence intervals) for core Fr10/95-GC17, plotted against sampling depth.

^{238}U, as expected for carbonaceous marine sediments (Ivanovich and Harmon, 1992), and are also in excess of the ^{230}Th concentrations in all of the samples.

Disequilibria in the ^{238}U decay series are well documented for deep-sea sediments (Ivanovich and Harmon, 1992). This gives rise to variations in radionuclide concentrations over time, with commensurate variations in the dose rates. Consequently, we have used an iterative model similar to those implemented by previous luminescence researchers (Wintle and Huntley, 1979, 1980; Stokes et al., 2003) to determine the effective dose rate for each sample integrated over the entire period of burial. The model allows for the in-growth of ^{230}Th and the decay of ^{234}U over the period of burial. For each sample, the measured radionuclide concentrations are initially used in conjunction with the D_e to provide a first approximation of the burial age. This age estimate is then used as the time interval over which the time-dependent variations in radionuclide concentrations are modelled to yield an improved, time-averaged, estimate of the dose rate. The latter is then used to calculate a second burial age for the sample, which is input to the model as a closer approximation of the true period of burial

Table 2
Sample water contents (% of dry weight), and lithogenic radionuclide concentrations and their standard errors (in Bq kg^{-1}), for each OSL sample from core Fr10/95-GC17

Sample	Water content (%)	^{238}U	^{234}U	$^{230}Th^{a}$	$^{232}Th^{b}$	^{40}K
OSL 1	105	46.2 ± 1.9	52.3 ± 2.1	26.9 ± 0.2	16.8 ± 0.5	209 ± 14
OSL 2	97	48.9 ± 1.9	54.3 ± 2.1	24.0 ± 0.6	20.7 ± 0.1	257 ± 16
OSL 3	95	40.0 ± 1.5	44.6 ± 1.6	27.5 ± 0.2	19.1 ± 0.2	240 ± 20
OSL 4	90	52.0 ± 4.0	59.8 ± 3.8	29.5 ± 0.4	2.7 ± 0.1	30 ± 3
OSL 5	88	48.0 ± 1.5	55.6 ± 1.4	29.9 ± 0.8	3.9 ± 0.5	33 ± 3
OSL 6	84	39.8 ± 1.3	47.2 ± 1.5	28.7 ± 0.7	5.1 ± 0.2	66 ± 7
OSL 7	80	44.7 ± 1.8	51.0 ± 2.0	37.3 ± 0.8	7.1 ± 0.4	96 ± 12

[a] Reported results are the weighted means of the measured concentrations of ^{230}Th, ^{226}Ra and ^{210}Pb, except for the near-surface sample (OSL 1), which had a ^{210}Pb excess of 12.9 ± 2.3 Bq kg^{-1}. The reported value for the latter sample is the weighted mean of the measured concentrations of ^{230}Th and ^{226}Ra.

[b] Reported results are the weighted means of the measured ^{232}Th, ^{228}Ra and ^{228}Th concentrations.

over which the dose rate should be adjusted for time-dependent variations in ^{230}Th and ^{234}U. This process is repeated until the changes in the estimated dose rate, and hence the burial age, become insignificant compared to their associated uncertainties. Correcting for the time-dependent variations in ^{230}Th and ^{234}U produced a decrease of 1–5% in the estimated dose rates, compared to the corresponding values obtained using the 'as measured' (present day) radionuclide concentrations. Following Wintle and Huntley (1980), we have also corrected the gamma dose rate for the rate of sediment accumulation (using the data in Table H.1 of Aitken, 1985), and the calculated effective fractions of the infinite matrix gamma dose for each OSL sample are reported in Table 3. The calculated total dose rates (D_r) are listed in Table 4.

5.2.2. OSL data

The single-grain D_e estimates for each of the samples are displayed in radial plots in Fig. 2. The over-dispersion parameter σ_d in Table 4 represents the relative standard deviation of the single-grain D_e distribution after having allowed for statistical estimation error. These values were obtained using the 'central age model' of Galbraith et al. (1999) to provide an estimate of the dispersion over and above the measurement error associated with each grain; if the latter were the only source of variation in D_e, then σ_d would be zero. Single-grain D_e estimates on natural samples are typically over-dispersed, with σ_d values of 9–22% for samples that are thought, or known, to have been well bleached at the time of deposition (Murray and Roberts, 1997; Roberts et al., 1998, 2000; Jacobs et al., 2003; Olley et al., in press; Galbraith et al., in press).

Table 3
The calculated effective fractions of the infinite matrix gamma dose for each OSL sample from core Fr10/95-GC17

Sample	K	Th	U
OSL 1	0.72	0.73	0.73
OSL 2	0.94	0.94	0.94
OSL 3	0.96	0.96	0.96
OSL 4	0.97	0.97	0.97
OSL 5	0.97	0.97	0.98
OSL 6	0.98	0.98	0.98
OSL 7	0.99	0.99	0.99

For the samples examined in this study, the σ_d values range from 0% to 34% (Table 4). Samples with over-dispersion values of less than 20% were considered to have been uniformly bleached at the time of deposition, and the central age model was used to determine the burial dose (D_b). However, samples OSL 5 and OSL 6 yielded σ_d values of 34% and 31%, respectively. The corresponding single-grain D_e values for sample OSL 5 ranged from 5.8 ± 1.8 to 40 ± 8 Gy, with a weighted mean of 11.2 ± 0.7 Gy (calculated using the central age model). And the D_e values for sample OSL 6 ranged from 7.9 ± 0.7 to 110 ± 20 Gy, with a weighted mean of 23.5 ± 0.9 Gy. The spread in D_e values from sample OSL 5 is similar to the 10–40 Gy spread in D_e reported for single grains from Holocene sediments considered to have been partially bleached at the time of deposition (Olley et al., in press); the ~ 100 Gy spread in D_e values from sample OSL 6 is the largest yet reported.

Table 4
Sampling depths, laboratory sample codes, percentage of grain with measurable D_e values, D_e over-dispersion (σ_d, in %), dose rates (D_r), burial dose estimates (D_b), and calculated burial ages for each OSL sample from core Fr10/95-GC17

Sampling depth (cm)	Laboratory sample code	Measurable grains (%)	Over-dispersion (%)	D_r (mGy year^{-1})	D_b (Gy)	Optical age (years)
7–8	OSL 1	37	12	0.76 ± 0.09	1.36 ± 0.15	1780 ± 290
57–58	OSL 2	94	0	0.91 ± 0.10	5.90 ± 0.12	6490 ± 730
83–84	OSL 3	23	9	0.84 ± 0.10	7.2 ± 0.4	8600 ± 1050
123–124	OSL 4	39	19	0.43 ± 0.06	7.71 ± 0.23	17,900 ± 2500
139–140	OSL 5	21	34	0.44 ± 0.07	8.3 ± 1.2	18,700 ± 3900
181–184	OSL 6	63	31	0.48 ± 0.06	15.3 ± 0.6	31,900 ± 4300
248.5–251.5	OSL 7	60	13	0.65 ± 0.08	33.2 ± 1.0	51,100 ± 6500

Several mechanisms have the potential to cause a spread in D_e values, including (i) beta dose heterogeneity (Olley et al., 1997; Nathan et al., 2003), (ii) partial bleaching (Olley et al., 1999, in press), and (iii) post-depositional disturbance, resulting in the intrusion of grains from underlying or overlying sediments (Roberts et al., 1999).

Close proximity of quartz grains to radioactive heavy minerals, such as zircons, would impart an enhanced beta dose (Roberts et al., 1999). Similarly, close proximity of grains to large, non-radioactive minerals (>1 mm in diameter) would result in their receiving a lower beta dose (Olley et al., 1997; Nathan et al., 2003). None of the OSL samples examined in this study contained dark-coloured minerals (indicative of some heavy minerals) and no heavy minerals (>2.70 g cm^{-3}) were obtained from density separation of the material collected from above and below sample OSL 6. The samples did, however, contain foraminiferal tests of ~ 300 μm in diameter. Uranium, thorium and potassium concentrations in foraminiferal tests are generally very low. If we assume that they are zero, where the effect would be at a maximum, a 300-μm-diameter test in contact with a 60-μm-diameter quartz grain would lower the effective beta dose by less than 10% in comparison to a grain surrounded entirely by fine sediment. Over a burial period of 30,000 years, the resulting difference in the total dose rate for individual grains would generate a spread of less than 1 Gy in the measured single-grain D_e values. From this calculation, and the absence of heavy minerals, we conclude that the spread in D_e observed in samples OSL 5 and OSL 6 is unlikely to have resulted from beta dose heterogeneity.

Comparison of D_e estimates obtained from the fast-dominated and slow-dominated components of the LM-OSL signal provides a means of assessing if grains were fully bleached at the time of deposition (Yoshida et al., 2003). The fast-dominated component is typically erased by a few seconds of exposure to sunlight (Aitken, 1998), whereas the slow-dominated component can take several hours or days to be fully reset (Singarayer et al., 2000). If grains were well bleached at the time of deposition, then the D_e estimates from both the fast- and slow-dominated components should be concordant (i.e., fast D_e/slow D_e ratios consistent with unity). By contrast, partial

Fig. 2. Radial plots (Galbraith, 1988) of the single-grain D_e estimates (Gy) for each of the OSL samples; the identifying numbers correspond to the OSL sample codes in Tables 2–4. The measured D_e (in Gy) for a grain can be read by tracing a line from the y-axis origin through the point until the line intersects the radial axis (log scale) on the right-hand side. The corresponding standard error for this estimate can be read by extending a line vertically to intersect the x-axis. The x-axis has two scales: one plots the relative standard error of the D_e estimate (in %) and the other ('Precision') plots the reciprocal standard error. Therefore, values with the highest precisions and the smallest relative errors plot closest to the radial axis on the right of the diagram, and the least precise estimates plot furthest to the left. The horizontal lines in the plots indicate the burial doses used to calculate the optical ages, and the shaded regions denote those data that are consistent with the burial doses at the 95% confidence interval. The burial doses for samples OSL 1–4 and OSL 7 were obtained using the central age model, while the burial doses of samples OSL 5 and OSL 6 were determined using the minimum age model; the central age model estimates for the latter two samples are shown as inclined thick black lines in the radial plots. The open triangles in box 6 denote the D_e estimates determined from the fast-dominated component of the LM-OSL emissions from individual grains of sample OSL 6.

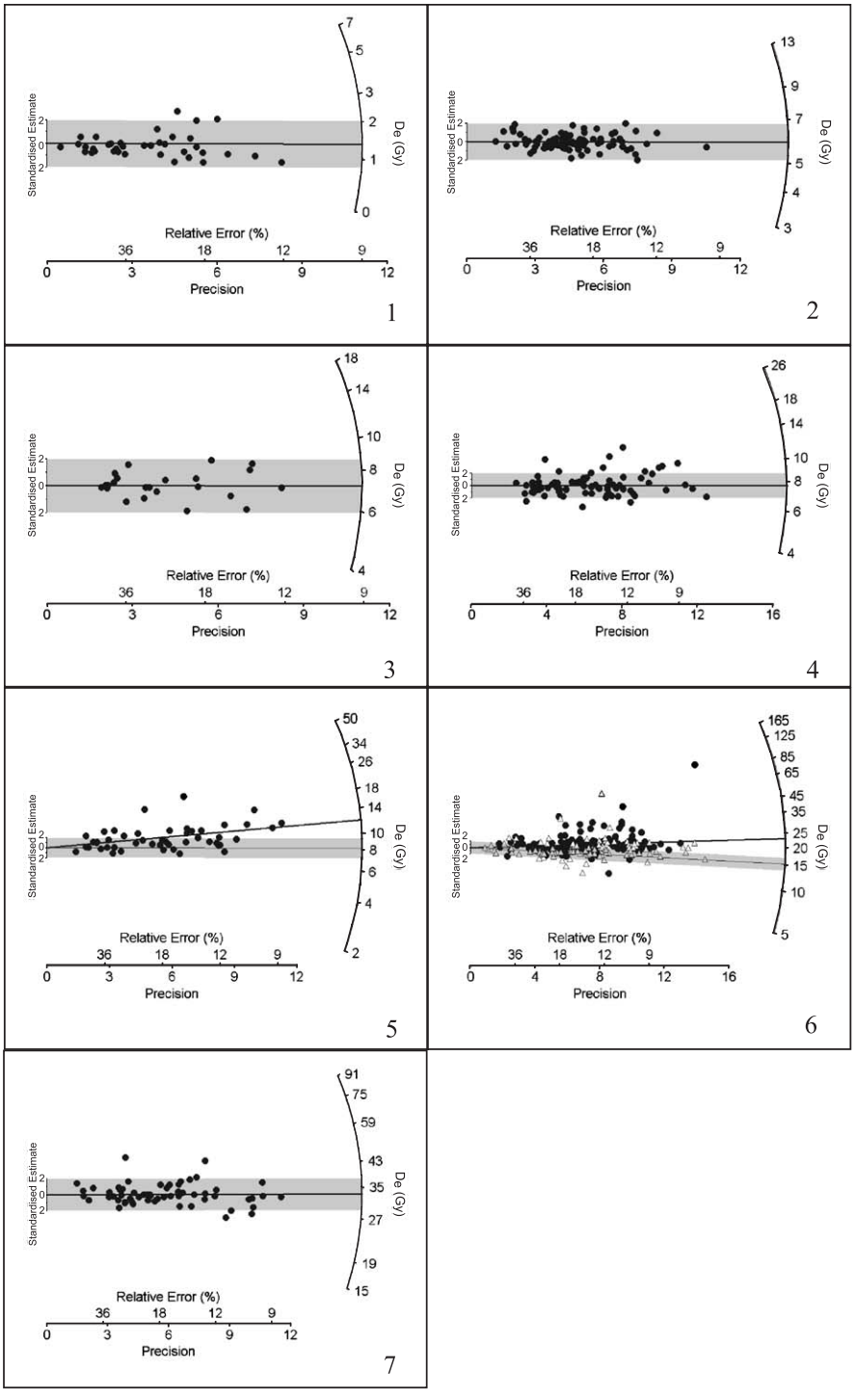
Standardised Estimate
De (Gy)
Relative Error (%)
Precision
1
2
3
4
5
6
7

bleaching would result in the D_e estimates from the fast-dominated component being lower than those obtained from the slow-dominated component (i.e., fast/slow ratios of <1). We measured 100 grains from sample OSL 6 using LM-OSL. The D_e estimates from the fast-component exhibit a similar range of values as those produced using continuous-wave OSL (Fig. 2, box 6). Of the measured grains, 75 produced measurable D_e values for both the fast- and slow-dominated components (with neither dose-response curve reaching saturation): 56 of these had fast/slow ratios consistent with unity at 2σ, while the remaining 19 grains had fast/slow ratios of less than 1, which we attribute to partial bleaching (Fig. 3). The continuous-wave OSL and LM-OSL data for sample OSL 6 both indicate that some of the constituent grains were insufficiently bleached at the time of deposition, and that marine sediments are not immune from partial or heterogeneous bleaching.

On the basis of this finding for sample OSL 6, we infer that the spread in single-grain D_e estimates for sample OSL 5 also results from partial bleaching. Consequently, we have used the 'minimum age model' of Galbraith et al. (1999) to estimate the burial dose for these two Pleistocene samples; Olley et al. (in press) have previously recommended use of this model for partially bleached Holocene sediments from a variety of depositional environments. The existence of incomplete or heterogeneous bleaching of the quartz grains means that any method that measures the D_e using a large number of grains (e.g., >100) in either single or multiple aliquots is likely to produce an overestimate of the true burial dose (Olley et al., 1999, in press).

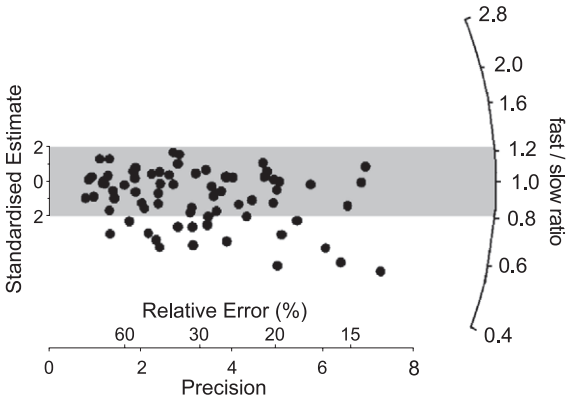

Fig. 3. Radial plot of the D_e ratios obtained from the fast- and slow-dominated LM-OSL components for 75 individual grains of quartz from sample OSL 6. Fifty-six of these ratios fall within the shaded region and are, therefore, consistent with unity at the 95% confidence interval.

The estimated burial doses are indicated by a thin horizontal line in each of the radial plots (Fig. 2) and are listed in Table 4, together with the calculated optical ages. For comparison, the central age model estimates of D_b for samples OSL 5 and OSL 6 are also shown (as inclined thick black lines) in Fig. 2.

5.2.3. Optical ages

The optical ages are in correct stratigraphic order (Table 4; Fig. 1) and range from 1780 ± 290 years to $51{,}100 \pm 6500$ years, with total relative uncertainties (at the 68% confidence interval) of between 11% and 21%. These uncertainties are significantly larger than those reported by Stokes et al. (2003) for optical ages of deep-sea sediments from the northwestern Indian Ocean, which ranged from 3% to 6%. Our analysis of the data presented by Stokes et al. (2003) indicates that their quoted uncertainties include only the random errors associated with the determination of the optical ages, whereas our reported uncertainties include both the random and systematic components. In any comparison of luminescence ages with independent chronologies, it is crucial that the uncertainties on the luminescence ages include contributions from all known components, including systematic uncertainties (see, for example, Appendix B of Aitken, 1985). It is the latter that, ultimately, limit the precision and accuracy attainable in luminescence dating (Murray and Olley, 2002). Some systematic uncertainties that are difficult to avoid include those associated with conversions from radionuclide concentration data to dose rates, the absolute calibration of the concentration measurements, the calibration of laboratory beta sources, and the determination of beta dose attenuation factors. Each of these uncertainties are of the order of $\sim 3\%$ (e.g., Aitken, 1985; Brennan, 2003). When other sources of systematic uncertainty, such as those associated with water content, are also propagated through to determine the total uncertainty on the age, it is difficult to obtain luminescence ages for deep-sea sediments with total relative uncertainties of much less than 10% at the 68% confidence interval. (For terrestrial and shallow marine sediments, it is

also necessary to include the systematic uncertainty associated with the cosmic-ray contribution to the dose rate, which may be of the order of ± 10%; Prescott and Hutton, 1994.) We note, however, that relative uncertainties of 10–20% of the mean age are similar to those associated with oxygen-isotope chronologies for the last 300,000 years (Martinson et al., 1987).

5.3. Comparison of optical and ^{14}C ages

The optical ages are plotted against the calibrated ^{14}C age ranges (at 1σ) in Fig. 4. We conducted a one-sample Student's *t*-test on the seven paired ^{14}C/OSL samples to determine if the differences between the ^{14}C and optical ages are significantly different from zero. To take account of the uncertainties associated with each sample age, we calculated a "standard normal" value; that is, the difference between the ^{14}C and optical ages for each sample, divided by the standard error of the difference, which was calculated as the square root of the sum of the squares of the two corresponding age uncertainties. A one-sample Student's *t*-test was then performed on the standard normal values to determine if they differed significantly from zero. There was no significant difference at the 95% confidence interval. Bearing in mind the uncertainties on both sets of ages, we conclude that there is no evidence for a systematic difference between the ^{14}C and OSL chronologies from ~ 1500 to 50,000 years ago.

The spread in single-grain D_e values for samples OSL 5 and OSL 6 is consistent with some of the quartz grains having been partially bleached at the time of deposition, and the LM-OSL data for sample OSL 6 support this inference. The poor bleaching of the grains may have arisen because of a surface coating on some of the grains or because they were transported at night; we consider it unlikely that the spread in D_e values is the result of beta dose heterogeneity. The weighted mean D_e estimates for samples OSL 5 (11.2 ± 0.7 Gy) and OSL 6 (23.5 ± 0.9 Gy)

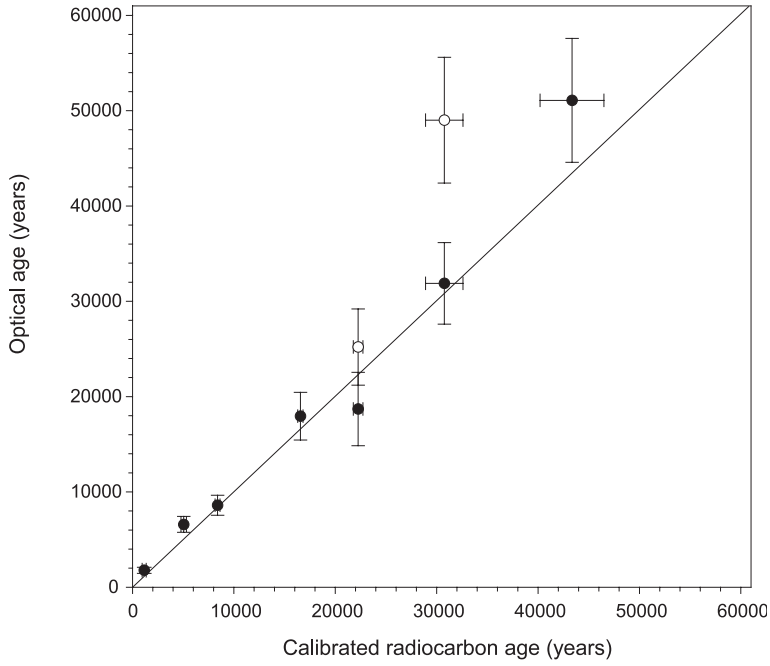

Fig. 4. Comparison of single-grain optical ages and calibrated ^{14}C ages. Error bars are at the 68% confidence interval. For samples OSL 5 and OSL 6, the filled circles represent the optical ages obtained from the burial doses estimated using the minimum age model, whereas the open circles denote the corresponding estimates obtained using the central age model. For all other samples, the filled circles denote the optical ages determined using the central age model estimates of the burial dose.

correspond to optical ages of 25,200 ± 4000 and 49,000 ± 6600 years, respectively (Fig. 4). The weighted mean age for sample OSL 5 is consistent with the calibrated ^{14}C age at the 1σ level, as is the optical age determined using the minimum age model. For sample OSL 6, however, the weighted mean age is inconsistent with the ^{14}C age, even at 2σ. For the latter sample, measuring the D_e distribution using single grains of quartz and employing the minimum age model to estimate the burial dose from the lowest population of D_e values is the best available means of obtaining a burial age that agrees with the ^{14}C chronology. This approach selects the most completely bleached grains for determination of the burial age. So too does the use of LM-OSL data obtained from grains with fast D_e/slow D_e ratios consistent with unity: the burial dose of 16.8 ± 0.8 Gy obtained using the minimum age model applied to the 56 such grains from sample OSL 6 (Fig. 3) corresponds to a burial age of 35,000 ± 4800 years, which agrees with the ^{14}C age at the 68% confidence interval.

The results for sample OSL 6 clearly show that heterogeneous bleaching of the optical dating signal can occur in marine sediments, and that aeolian transport of grains prior to fallout in the ocean does not guarantee that all grains will be well bleached at the time of deposition. To have confidence in optical ages for marine sediments, we recommend that samples be routinely checked for partial or heterogeneous bleaching by measuring single grains, or small aliquots, of quartz and explicitly determining the extent of any D_e over-dispersion. In cases where the data over-dispersion suggests partial or heterogeneous bleaching of the OSL signal (σ_d>20% for single grains), the minimum age model should be used to estimate the burial dose from the lowest D_e population. For samples that appear to have been well bleached at the time of deposition (σ_d < 20% for single grains), the central age model should be used to calculate the burial dose.

5.4. Maximum age limit for optical dating

The upper age limit of optical dating depends on both the environmental dose rate and the dose at which the quartz grains reach saturation (Yoshida et al., 2000). Fig. 5 shows the regenerated dose-response curves (up to 130 Gy) for four grains typical of those examined in this study. Within the range of applied doses, only one of these (grain 4) has attained dose-saturation (at ~ 100 Gy). Most of the grains examined were not saturated at applied doses of 130

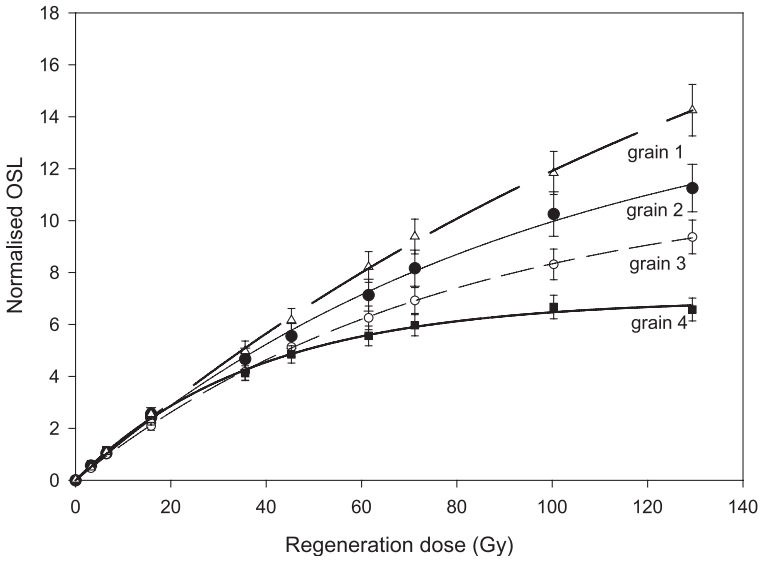

Fig. 5. Regenerated dose-response curves (up to 130 Gy) for four grains typical of those examined in this study. Grains 1, 2, 3 and 4 are from samples OSL 1, 4, 5 and 7, respectively. Error bars are at the 68% confidence interval.

Gy. Dose rates in the samples from the core ranged from 0.43 to 0.91 mGy year^{-1}, corresponding to an age range of ~140,000 to ~300,000 years for grains with D_b values of 130 Gy. The fitted curves in Fig. 5 indicate that grains 1–3 would be saturated at doses of 250–300 Gy, which would enable optical ages to be obtained for sediments deposited up to 700,000 years ago. The uncertainties associated with curve fitting and interpolation of the natural dose increase for samples that are close to saturation. These expanded random uncertainties, taken together with the above discussion on the various systematic uncertainties associated with optical dating, render it unlikely that samples approaching or exceeding 500,000 years in age can be dated with a precision of better than ~20%.

6. Conclusions

We conclude that optical dating using single grains of quartz offers an alternative and accurate means of dating deep-sea sediments deposited up to 500,000 years ago, or possibly longer. At present, however, the random and systematic uncertainties associated with optical dating of marine sediments are sufficiently large as to preclude age determinations with total uncertainties of less than ~10%; relative uncertainties of this size are, nonetheless, of comparable precision to those associated with Late Quaternary oxygen-isotope chronologies. We had intended to use the optical ages to examine past changes in the marine carbon reservoir, but this objective was precluded by the size of the uncertainties associated with the optical ages.

It is also concluded that heterogeneous bleaching of the optical dating signal occurs in marine sediments, and that aeolian transport of sediment prior to deposition in the marine environment is not a sufficient guarantee that all grains will have been adequately bleached at the time of deposition. Samples should, therefore, be routinely checked for partial or heterogeneous bleaching to provide confidence in optical age determinations for marine sediments. Where partial or heterogeneous bleaching of the OSL signal is indicated, single-grain dating should be employed and the minimum age model (Galbraith et al., 1999) used to estimate the burial dose from the population of grains with the smallest D_e values. For well-bleached samples, the central age model (Galbraith et al., 1999) is recommended, as this takes into account any D_e dispersion over and above the measurement error associated with each grain.

Acknowledgements

We thank Jacqui Olley for OSL sample preparation, Chris Leslie for gamma spectrometry analyses, Melissa Dobbie for statistical support, and ANSTO (AINSE grant 97/057R awarded to De Deckker), Hokkaido University and Monash University for funding the ^{14}C age determinations. Roberts and Yoshida thank the Australian Research Council for the support of a Senior Research Fellowship and a Postdoctoral Research Fellowship, respectively. T. Barrows is thanked for comments on the errors associated with oxygen-isotope chronologies, and D. Huntley, S. Stokes, J. Wallinga and A. Murray are thanked for reviews of this work, which improved the manuscript.

References

Aitken, M.J., 1985. Thermoluminescence Dating. Academic Press, London. 359 pp.

Aitken, M.J., 1998. An Introduction to Optical Dating. Oxford Univ. Press, Oxford. 267 pp.

Berger, G.W., Huntley, D.J., Stipp, J.J., 1984. Thermoluminescence studies on a ^{14}C-dated marine core. Canadian Journal of Earth Sciences 21, 1145–1150.

Brennan, B.J., 2003. Beta doses to spherical grains. Radiation Measurements 37, 299–303.

Bowler, J.M., 1978. Glacial age aeolian events at high and low latitudes: a Southern Hemisphere perspective. In: van Zinderen Bakker, E.M. (Ed.), Antarctic Glacial History and World Paleoenvironments. Balkema, Rotterdam, pp. 149–172.

Bowler, J.M., Johnston, H., Olley, J.M., Prescott, J.R., Roberts, R.G., Shawcross, W., Spooner, N.A., 2003. New ages for human occupation and climatic change at Lake Mungo, Australia. Nature 421, 837–840.

De Deckker, P., 2001. Records of environmental changes in the Australian sector of PEP II point to broad trends of climate change. PAGES News 9, 4–5.

Galbraith, R.F., 1988. Graphical display of estimates having differing standard errors. Technometrics 30, 271–281.

Galbraith, R.F., Roberts, R.G., Laslett, G.M., Yoshida, H., Olley, J.M., 1999. Optical dating of single and multiple grains of

quartz from Jinmium rock shelter, northern Australia: Part I, experimental design and statistical models. Archaeometry 41, 339–364.

Galbraith, R.F., Roberts, R.G., Yoshida, H., 2004. Error variation in OSL palaeodose estimates from single aliquots of quartz: a factorial experiment. Radiation Measurements (in press).

Gingele, F.X., De Deckker, P., Hillenbrand, C.D., 2001. Late Quaternary fluctuations of the Leeuwin Current and palaeoclimates on the adjacent land masses: clay mineral evidence. Australian Journal of Earth Sciences 48, 867–874.

Harrison, S.P., Kohfeld, K.E., Roelandt, C., Claquin, T., 2001. The role of dust in climate changes today, at the last glacial maximum and in the future. Earth-Science Reviews 54, 43–80.

Henderson, G.M., Slowey, N.C., 2000. Evidence from U–Th dating against Northern Hemisphere forcing of the penultimate deglaciation. Nature 404, 61–66.

Hesse, P.P., McTainsh, G.H., 2003. Australian dust deposits: modern processes and the Quaternary record. Quaternary Science Reviews 22, 2007–2035.

Hughen, K., Lehman, S., Southon, J., Overpeck, J., Marchal, O., Herring, C., Turnbull, J., 2004. ^{14}C activity and global carbon cycle changes over the past 50,000 years. Science 303, 202–207.

Huntley, D.J., Godfrey-Smith, D.L., Thewalt, M.L.W., 1985. Optical dating of sediments. Nature 313, 105–107.

Huntley, D.J., Hutton, J.T., Prescott, J.R., 1993. Optical dating using inclusions within quartz grains. Geology 21, 1087–1090.

Ivanovich, M., Harmon, R.S., 1992. Uranium-series Disequilibrium: Applications to Earth, Marine, and Environmental Sciences, 2nd ed. Clarendon Press, Oxford. 910 pp.

Jacobs, Z., Duller, G.A.T., Wintle, A.G., 2003. Optical dating of dune sand from Blombos Cave, South Africa: I-single grain data. Journal of Human Evolution 44, 613–625.

Jennings, J.N., 1968. A revised map of the desert dunes of Australia. Australian Geographer 10, 408–409.

Laj, C., Kissel, C., Mazaud, A., Michel, E., Muscheler, R., Beer, J., 2002. Geomagnetic field intensity, North Atlantic deep water circulation and atmospheric $\Delta^{14}C$ during the last 50 kyr. Earth and Planetary Science Letters 200, 177–190.

Martin, P., Hancock G., 1992. Routine analysis of naturally occurring radionuclides in environmental samples by alpha-particle spectrometry. Research Report 7, Supervising Scientist for the Alligator Rivers Region, Australia Government Printing Service, Canberra.

Martinez, I., De Deckker, P., Barrows, T., 1999. Palaeoceanography of the last glacial maximum in the eastern Indian Ocean: planktonic foraminiferal evidence. Palaeogeography, Palaeoclimatology, Palaeoecology 147, 73–99.

Martinson, D.G., Pisias, N.G., Hays, J., Imbrie, J., Moore, T.C., Shackleton, N.J., 1987. Age dating and the orbital theory of the ice ages: development of a high-resolution 0 to 300,000 year chronology. Quaternary Research 27, 1–29.

Mejdahl, V., 1979. Thermoluminescence dating: beta-dose attenuation in quartz grains. Archaeometry 21, 61–72.

Murgese, S.D., 2003. Late Quaternary palaeoceanography of the eastern Indian Ocean based on benthic foraminifera. PhD thesis, Australian National University, Canberra. 177 pp.

Murray, A.S., Olley, J.M., 2002. Precision and accuracy in the optically stimulated luminescence dating of sedimentary quartz: a status review. Geochronometria 21, 1–16.

Murray, A.S., Roberts, R.G., 1997. Determining the burial time of single grains of quartz using optically stimulated luminescence. Earth and Planetary Science Letters 152, 163–180.

Murray, A.S., Marten, R., Johnston, A., Martin, P., 1987. Analysis for naturally occurring radionuclides at environmental concentrations by gamma spectrometry. Journal of Radioanalytical and Nuclear Chemistry 115, 263–288.

Nathan, R.P., Thomas, P.J., Jain, M., Murray, A.S., Rhodes, E.J., 2003. Environmental dose rate heterogeneity of beta radiation and its implications for luminescence dating: Monte Carlo modelling and experimental validation. Radiation Measurements 37, 305–313.

Ohkouchi, N., Eglinton, T.I., Keigwin, L.D., Hayes, J.M., 2002. Spatial and temporal offsets between proxy records in a sediment drift. Science 298, 1224–1227.

Olley, J.M., Roberts, R.G., Murray, A.S., 1997. Disequilibria in the uranium decay series in sedimentary deposits at Allen's Cave, Nullarbor Plain, Australia: implications for dose rate determinations. Radiation Measurements 27, 433–443.

Olley, J.M., Caitcheon, G., Murray, A.S., 1998. The distribution of apparent dose as determined by optically stimulated luminescence in small aliquots of fluvial quartz: implications for dating young sediments. Quaternary Science Reviews 17, 1033–1040.

Olley, J.M., Caitcheon, G.G., Roberts, R.G., 1999. The origin of dose distributions in fluvial sediments, and the prospect of dating single grains of quartz from fluvial deposits using optically stimulated luminescence. Radiation Measurements 30, 207–217.

Olley, J.M., Pietsch, T., Roberts, R.G., 2004. Optical dating of Holocene sediments from a variety of geomorphic settings using single grains of quartz. Geomorphology, 60, 337–358.

Prescott, J.R., Hutton, J.T., 1994. Cosmic ray contributions to dose rates for luminescence and ESR dating: large depths and long-term time variations. Radiation Measurements 23, 497–500.

Roberts, R., Yoshida, H., Galbraith, R., Laslett, G., Jones, R., Smith, M., 1998. Single-aliquot and single-grain optical dating confirm thermoluminescence age estimates at Malakunanja II rock shelter in northern Australia. Ancient TL 16, 19–24.

Roberts, R.G., Galbraith, R.F., Olley, J.M., Yoshida, H., Laslett, G.M., 1999. Optical dating of single and multiple grains of quartz from Jinmium rock shelter, northern Australia: Part II, results and implications. Archaeometry 41, 365–395.

Roberts, R.G., Galbraith, R.F., Yoshida, H., Laslett, G.M., Olley, J.M., 2000. Distinguishing dose populations in sediment mixtures: a test of single-grain optical dating procedures using mixtures of laboratory-dosed quartz. Radiation Measurements 32, 459–465.

Sikes, E.L., Samson, C.R., Guilderson, T.P., Howard, W.R., 2000. Old radiocarbon ages in the southwest Pacific Ocean during the last glacial period and deglaciation. Nature 405, 555–559.

Singarayer, J.S., Bailey, R.M., 2003. Further investigations of the quartz optically stimulated luminescence components using linear modulation. Radiation Measurements 37, 451–458.

Singarayer, J.S., Bailey, R., 2004. Component-resolved bleaching spectra of quartz optically stimulated luminescence: preliminary results and implications for dating. Radiation Measurements 38, 111–118.

Singarayer, J.S., Bailey, R.M., Rhodes, E.J., 2000. Potential of the slow component of quartz OSL for age determination of sedimentary samples. Radiation Measurements 32, 873–880.

Stokes, S., Ingram, S., Aitken, M.J., Sirocko, F., Anderson, R., Leuschner, D., 2003. Alternative chronologies for late quaternary (Last Interglacial–Holocene) deep sea sediment via optical dating of silt-size quartz. Quaternary Science Reviews 22, 925–941.

Stuiver, M., Reimer, P.J., Beck, J.W., Bard, E., Burr, G.S., Hughen, K.A., Kromer, B., McCormack, F.G., van der Plicht, J., Spurk, M., 1998. INTCAL98 radiocarbon age calibration, 24,000–0 cal BP. Radiocarbon 40, 1041–1083.

Takahashi, K., Okada, H., 2000. The paleoceanography for the last 30,000 years in the southeastern Indian Ocean by means of calcareous nannofossils. Marine Micropaleontology 40, 83–103.

Truscott, A.J., Duller, G.A.T., Bøtter-Jensen, L., Murray, A.S., Wintle, A.G., 2000. Reproducibility of optically stimulated luminescence measurements from single grains of Al_2O_3:C and annealed quartz. Radiation Measurements 32, 447–451.

van der Kaars, S., De Deckker, P., 2002. A Late Quaternary pollen record from deep-sea core Fr10/95, GC17 offshore Cape Range Peninsula, northwestern Western Australia. Review of Palaeobotany and Palynology 120, 17–39.

Wintle, A.G., 1997. Luminescence dating: laboratory procedures and protocols. Radiation Measurements 27, 769–817.

Wintle, A.G., Huntley, D.J., 1979. Thermoluminescence dating of a deep-sea sediment core. Nature 279, 710–712.

Wintle, A.G., Huntley, D.J., 1980. Thermoluminescence dating of ocean sediments. Canadian Journal of Earth Sciences 17, 348–360.

Yoshida, H., Roberts, R.G., Olley, J.M., Laslett, G.M., Galbraith, R.F., 2000. Extending the age range of optical dating using single 'supergrains' of quartz. Radiation Measurements 32, 439–446.

Yoshida, H., Roberts, R.G., Olley, J.M., 2003. Progress towards single-grain optical dating of fossil mud-wasp nests and associated rock art in northern Australia. Quaternary Science Reviews 22, 1273–1278.